Journal of Applied Polymer Science

Electrical conductivity and electromagnetic interference shielding effectiveness of carbon black/sisal fiber/polyamide/polypropylene composites

Hezhi He, Shuwen Cheng, Yeqi Lian, Yue Xing, Guangjian He, Zhaoxia Huang, Mingchun Wu
The Key Laboratory of Polymer Processing Engineering, Ministry of Education, National Engineering Research Center of Novel Equipment for Polymer Processing, South China University of Technology, Guangzhou 510640, China
Correspondence to: H. He (E-mail: pmhzhe@scut.edu.cn)

ABSTRACT: The effects of hybrid fillers on the electrical conductivity and electromagnetic interference (EMI) shielding effectiveness (SE) of polyamide 6 (PA6)/polypropylene (PP) immiscible polymer blends were investigated. Carbon black (CB) and steam exploded sisal fiber (SF) were used as fillers. CB was coated on the surface of SF, and this was exploded by water steam to form carbon black modified sisal fiber (CBMSF). CB/SF/PA6/PP composites were prepared by melt compounding, and its electromagnetic SE was tested in low-frequency and high-frequency ranges. We observed that SF greatly contributed to the effective decrease in the percolation threshold of CB in the PA6/PP matrix and adsorbed carbon particles to form a conductive network. Furthermore, an appropriate CB/SF ratio was important for achieving the best shielding performance. The results indicate that CBMSF was suitable for use as electronic conductive fillers and the CB/SF/PA6/PP composites could be used for the purpose of EMI shielding. © 2015 Wiley Periodicals, Inc. J. Appl. Polym. Sci. **2015**, *132*, 42801.

KEYWORDS: carbon black; composite; electromagnetic interference shielding; sisal fiber; steam explosion

Received 14 May 2015; accepted 4 August 2015
DOI: 10.1002/app.42801

INTRODUTION

In the last few decades, with the great progress in modern technology, especially the rapid development of the electronics and telecommunication industry, electric and electronic devices have been widely used all over the world. However, the serious pollution produced by those devices, such as electromagnetic interference (EMI) and electromagnetic radiation, has been destroying the environment and even threatening human life.[1] Consequently, the fabrication of electromagnetic interference shielding composites (ESCs) has been a top focus in the study of environmental protection materials.[2]

Carbon black (CB) is one of commonly used conductive fillers in ESCs because it has a superior conductivity.[3–5] The CB-filled polymer matrix ESC has many good properties, such as a light weight, corrosion resistance, and easy formation process; it has become a hot spot in current research.[6–9] For CB-filled ESC, their electromagnetic shielding properties often depend on the features of the polymer matrix (e.g., chemical groups and surface tension) and CB (e.g., species, surface area, and degree of dispersion).[10,11] The distribution of CB particles in the composites affects many properties of the polymer matrix ESC significantly, especially the percolation threshold.[9,12,13] According to the percolation theory, the *percolation threshold* refers to the critical volume fraction of CB in the materials to form interconnected conductive networks, at which the electrical conductivity of the materials increases abruptly, and the insulator–conductor transition appears.[14–16]

Recently, studies of polymers reinforced with natural fibers have become a subject of increasing interest because of the demand on the protection of natural resources.[17–21] Sisal fiber (SF), as a kind of natural plant fiber, has annual output amounts of 4.5 megatons all over the world. It is commonly used in polymer composites because of its low cost, low density, high specific strength and modulus, no health risk, and easy availability. However, compatibility between hydrophilic natural fibers and hydrophobic polymers is so poor that most performance of the composites cannot meet the requirements in applications.[22]

Steam explosion is a new technology for pretreating plant fibers; it has developed rapidly in recent years and has lots of advantages, including a low cost and nonpollution. According to reports in some literature, steam explosions can make SF thinner, increase the specific surface, and reduce the bonding force among plant fiber bundles.[23]

In this study, we examined the effect of the CB/SF mass ratio of the carbon black modified sisal fiber (CBMSF) content on the shielding effectiveness (SE) tested in the screened room. Furthermore, microstructural pictures were used to observe the distribution of CB and CBMSF.[24–26] In the CB/SF/polyamide 6 (PA6)/polypropylene (PP) composites, CB was distributed in the polymer matrix and on the surface of SF. The distribution of CB on SF constituted microconductive chains, and then, the chains overlapped each other to form macroconductive networks.

EXPERIMENTAL

Materials

PP (TS30) was supplied from Maoming Petroleum Chemical Co. (Maoming, China), and PA6 (1013B) was obtained from Ube Industries Co. (Japan). Conductive CB (3000 meshes) was purchased from Cabot Co. SFs were purchased from Guangdong Dong Fang Sisal Co., Ltd. (Zhanjiang, China). NaOH powders were purchased from Tianjin Dalu Chemical Reagent Factory (Tianjin, China). Solutions of 10 wt % NaOH were prepared in an aquarium with a capacity of 10 L. Ethyl alcohol (95%) was supplied by Tianjin Fu Yu Chemical Co., Ltd. (Tianjin, China). Guangzhou Ju Cheng Zhao Ye Organic Silicon Material Center (Guangzhou, China) offered the silane coupling agents (KH550). The primary antioxidant (1010) and subsidiary antioxidant (168) were supplied from Dongguan De Ji Chang Plastic Material Co., Ltd. (Dongguan China).

Pretreatment of the SFs

SF bundles were cut into 4-mm short fibers and then soaked in a 10 wt % NaOH solution for 8 h. The treated SFs were rinsed with distilled water until the pH of the fibers was 7 (the test strips were put in the washing water when the color of strip was same as the referent color when the pH was 7). Then, soppy SF was dried under the condition of 80°C for 8 h. After drying, distilled water was sprayed onto the fibers until the water content was about 50%. Subsequently, a steam explosion machine was used to blast the SF into cotton wool shapes. All of the blasted fibers were dried under the condition of 80°C by an oven for 8 h.

Preparation of the Modified SFs

Silane coupling agents (KH550) in 2 wt % ethanol solutions were gently sprayed onto the SF surface and then reacted adequately in a high-speed mixer for 10 min. Subsequently, conductive CB was put into the mixer and blended with fibers for 10 min. All of the mixtures were dried under the condition of 80°C in an oven for 6 h before use. The final products were appointed as CBMSF.

Preparation of the Samples

CBMSF and PP were compounded together in proportion by a two-roll open mixing mill and then granulated. PA6 was mixed with the granulated particles in the high-speed mixer for 10 min. After mixing, the CB/SF/PA6/PP composites were extruded in a triple-screw extruder and made into particles. The CB/SF/PA6/PP particles were hot-pressed into to quadrate plates ($3 \times 280 \times 280$ mm^3) by compression modeling.

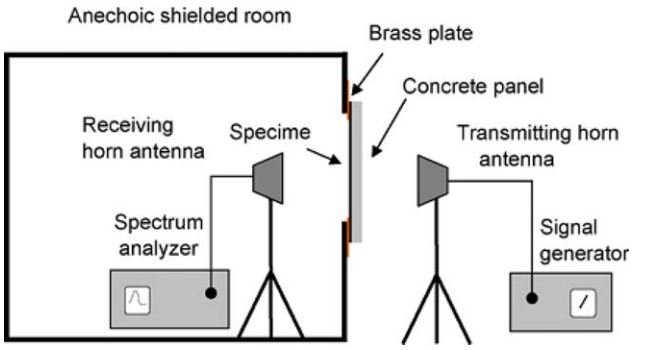

Figure 1. Schematic diagram of the screened room method. [Color figure can be viewed in the online issue, which is available at wileyonlinelibrary.com.]

Measurement of the Electrical Conductivity and SE

The CB/SF/PA6/PP composite square specimens were cut into disks that were 100 mm in diameter and 3 mm in thickness. The electrical conductivity of the disks was tested with a four-probe tester (RTS-9, GuangZhou 4 Probes Technology, the measurable conductivity range was from 10^{-5} to 10^{5} S/cm) when the material resistance was less than 10^{6} ohm and a ZC36 high-resistance instrument (Shanghai Precision Instruments Co., Ltd.) when the material resistance was in the range from 1×10^{6} to 1×10^{17} ohm.[27] All of the data were taken as averages of three test specimens.

The electromagnetic SE of the CB/SF/PA6/PP composite quadrate plates were measured by the screened room method (Figure 1). The setup of the SE measurement was composed of an anechoic shielded room, a signal generator (Agilent E8257D-532), a spectrum analyzer (Agilent 4408B), and transmitting and receiving antennas. The distance between the two antennas was 2.0 m, and the samples were pressed against the brass plate. The electromagnetic frequency range was from 400 MHz to 18 GHz.[28–30]

RESULTS AND DISCUSSION

Microstructural Analysis

At first, SF is a type of leaf fiber crop. The untreated SF used here was in the form of fiber bundles 50 μm in diameter, which contained many fiber cells glued together. The morphology of the untreated SF is shown in Figure 2(a). Compared with the untreated SF, the blasted SF was slender, flexible, and easily deformed, as shown in Figure 2(b).[31] The average fiber width was 15 μm, and the length of fibers almost had no changes. The specific surface area of SF increased substantially. At the same time, cells other than fiber cells that had thinner cell walls were destroyed into many floss-shaped microfibers, which had a high surface activity. Figure 2(c) shows that the CB coated on the surface of the blasted SF still existed after blending. The coating mechanism was mainly twofold. On the one hand, the hydrogen bonds between the intramolecular and intermolecular chains of cellulose and hemicellulose were destroyed in the process of steam explosion because of the high temperature and high pressure. A mass of free hydroxyl groups was generated, so the surface activity of SF was strengthened. On the other hand, the coupling agent could act as a bridge. The organic functional

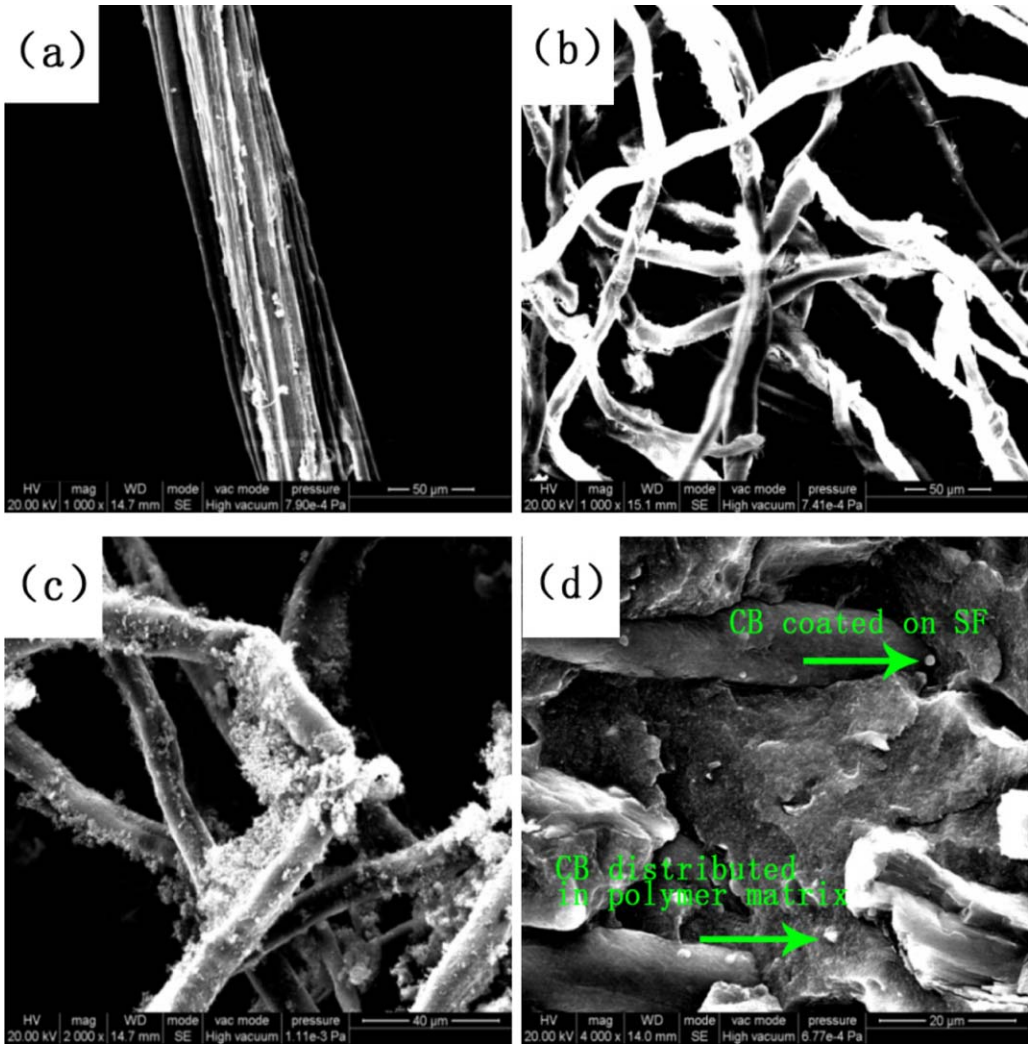

Figure 2. Microstructures (scanning electron microscopy) of the (a) untreated SF, (b) blasted SF, (c) CBMSF, and (d) CB/SF/PA6/PP composites. [Color figure can be viewed in the online issue, which is available at wileyonlinelibrary.com.]

groups and silanol groups of the coupling agent could combine with the blasted SF and inorganic fillers, respectively.

As shown in Figure 2(d), CB was not only coated on SF but was also distributed in the polymer matrix. Therefore, the main reason that SF could obviously increase the direct current conductivity and SE of the composites was that the CBMSF, which overlapped each other, could form a conductive network. Moreover, SF occupied a part of the volume and thus raised the volume fraction of CB and increased the number of microconductive chains in the polymer matrix.

Electrical Conductivity Analysis

The electrical conductivity of the conductive composites was related to the mass fractions of CB and CBMSF, as shown in Figure 3 and Table I. The results of the electrical conductivity of the CB/PA6/PP composites show that when the CB content was less than 10 wt %, the electrical conductivity of the CB/PA6/PP composites was below 10^{-7} S/m and changed slightly. When the CB content was 10–15 wt %, the electrical conductivity of the

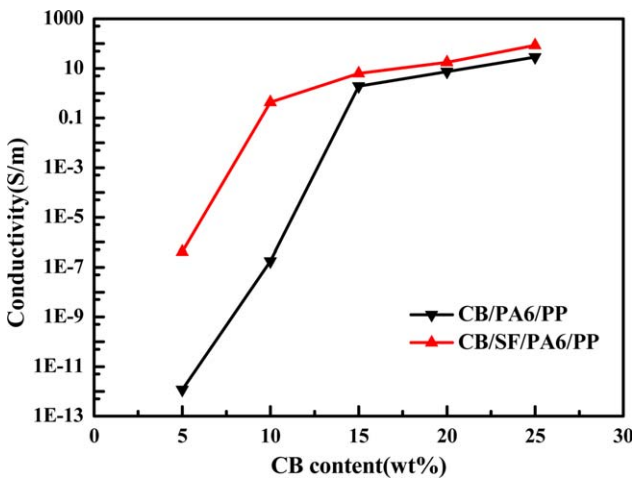

Figure 3. Effect of the CB content on the electrical conductivity of the CB/PA6/PP and CB/SF/PA6/PP composites (CB/SF mass ratio = 1 : 1 and PA6/PP mass ratio = 1 : 4). [Color figure can be viewed in the online issue, which is available at wileyonlinelibrary.com.]

Table I. Electrical Conductivity of the CB/SF/PA6/PP Composites

Component	Electrical conductivity (S/m)
25% CB, 2 : 1 CB:SF, 1 : 4 PA6/PP	5.61×10^1
25% CB, 1 : 1 CB/SF, 1 : 4 PA6/PP	8.58×10^1
25% CB, 2 : 3 CB/SF, 1 : 4 PA6/PP	6.61×10^1

CB/PA6/PP composites increased dramatically (~7 orders of magnitude) with CB content. This phenomenon is known as the *percolation effect*, and this CB content (10–15 wt %) is called the *percolation threshold*. However, at a CBMSF content of 10–20 wt %, which was equivalent to a CB content of 5–10 wt %, the electrical conductivity of the CB/SF/PA6/PP composites increased significantly. That is, the CB content 5–10 wt % was the percolation threshold of the CB/SF/PA6/PP composites. In contrast, the percolation thresholds of CB in the CB/PA6/PP and CB/SF/PA6/PP compostites, with the addition of SF, which constituted the basic skeleton of the conductive network, decreased effectively in the PA6/PP matrix. The main reason for this behavior was the formation of an interconnected conductive network by CBMSF, which overlapped with each other. Moreover, as the microconductive chains in the matrix connected with the conductive network of CBMSF, the conductive paths increased significantly in the PA6/PP matrix. So, with the combined effect of the formation of many conductive paths and the tunneling effect of the gap between the paths, the mutation area of the electrical conductivity of the CB/SF/PA6/PP composites with increasing CB content appeared relatively earlier compared with the CB/PA6/PP composites.[32] Thus, we proposed that the addition of SF to the matrix decreased the dose of CB, and the electrical conductivity of the CB/SF/PA6/PP composites still remained high.

Table I indicates that the electrical conductivity of the CB/SF/PA6/PP composites achieved a maximum when the mass ratio of SF/CB was 1 : 1. It was evident that when the SF/CB ratio was moderate, CBMSF could form good conductive networks.

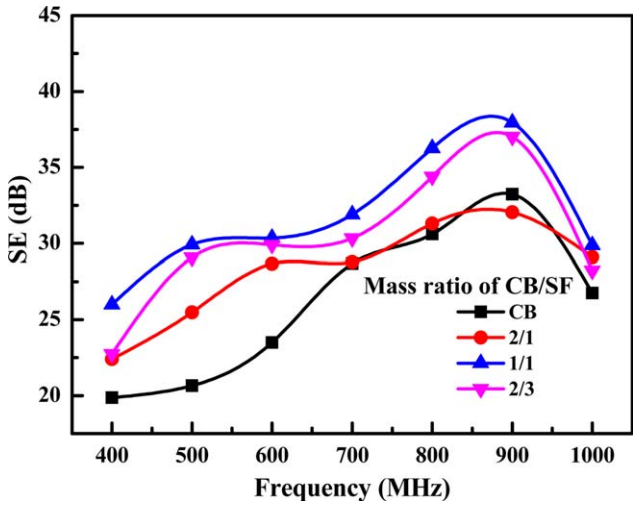

Figure 4. Effect of the CB/SF mass ratio on SE in the low-frequency range (CB, 25 wt %; PA6/PP mass ratio = 1 : 4). [Color figure can be viewed in the online issue, which is available at wileyonlinelibrary.com.]

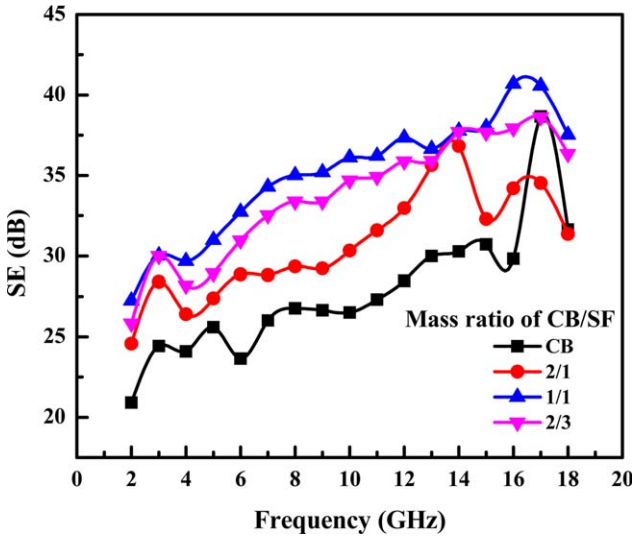

Figure 5. Effect of the CB/SF mass ratio on SE in the high-frequency range (CB, 25 wt %; PA6/PP mass ratio = 1:4). [Color figure can be viewed in the online issue, which is available at wileyonlinelibrary.com.]

Electromagnetic SE Analysis

Figures 4 and 5 show the relationship between the CB/SF mass ratio and SE of the composites when the CB content was 25 wt %, and the mass ratio of PA6/PP was 1 : 4 in low- and high-frequency ranges, respectively. With decreasing CB/SF mass ratio, SE increased in the beginning and then decreased rapidly. When the CB/SF mass ratio was 1 : 1 (the CB and SF content were both 25 wt %), the best SE was achieved; it reached up to 38 dB (900 MHz) in low-frequency range and 40.7 dB (16 GHz) in the high-frequency range. Under a constant CB content and PA6/PP mass ratio, the addition of CBMSF in the composites promoted SE of composites obviously in both the low-frequency and high-frequency ranges. This effect of CBMSF could be summarized by the following two aspects. On the one hand, part of the CB particles were adsorbed onto the SF surface to form the so-called conductive SFs, which overlapped together in the matrix to form conductive networks. On the other hand, the addition of SFs occupied a portion of the composite volume and then increased the concentration of CB in the polymer matrix; this raised the possibility of the formation of microconductive chains.

Figures 6 and 7 display the relationship between the CBMSF content and SE of the composites when the mass ratios of CB to SF was 1 : 1 and that of PA6 to PP was 1 : 4 at low and high frequencies, respectively. The SE of the composites increased with increasing CBMSF content. In the low-frequency range, when the CBMSF content was above 20 wt %, the SE of composites increased substantially. A concentration of 20 wt % was considered the percolation threshold of the composites. Similarly, in the high-frequency range, 30 wt % was considered to be the percolation threshold of the composites. The higher SE obtained in this study was attributed to the efficient formation of conductive networks by CBMSF. Finally, the target value of

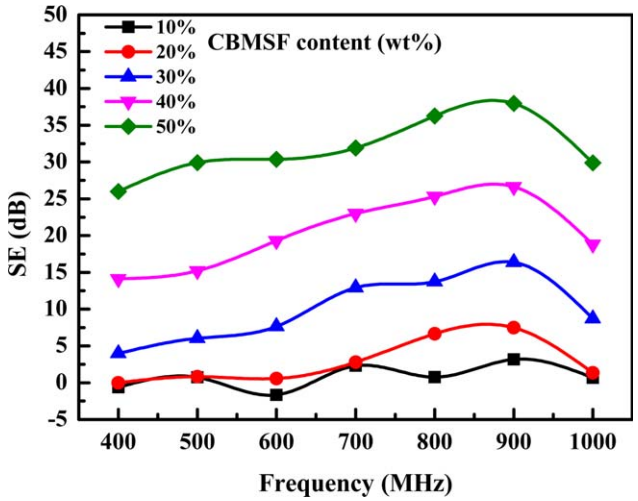

Figure 6. Effect of the CBMSF content on SE in the low-frequency range (CB/SF mass ratio = 1 : 1 and PA6/PP mass ratio = 1 : 4). [Color figure can be viewed in the online issue, which is available at wileyonlinelibrary.com.]

the SE needed for civil use (~30 dB) was obtained at a 50 wt % CBMSF loading in the PA6/PP matrix.[33,34]

For flat electromagnetic shielding material, the Schelkunoff formula is usually adopted in the theoretical calculation of SE.[35] The Schelkunoff formula was expressed as follows:

$$SE = SE_A + SE_R + SE_{MR} \quad (1)$$

where SE is the total shielding effectiveness and SE_A, SE_R, and SE_{MR} represent the electromagnetic wave absorption dissipation, electromagnetic wave reflection dissipation on the surface of the material, and the electromagnetic wave multiple reflections dissipation inside the material, respectively.

The calculation of SE_A, SE_R, and SE_{MR} is as follows:

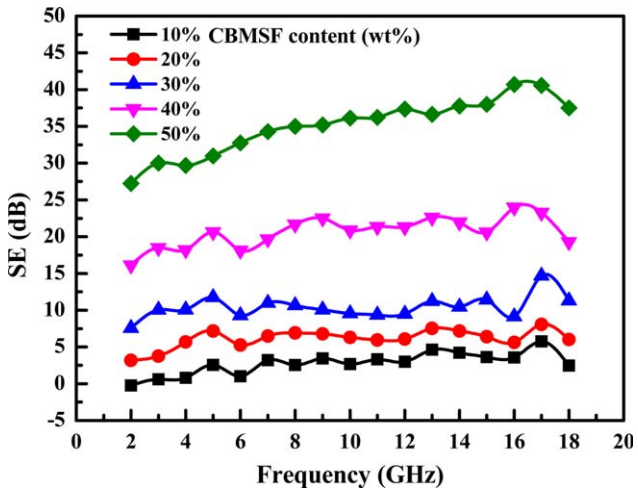

Figure 7. Effect of the CBMSF content on SE in the high-frequency range (CB/SF mass ratio = 1 : 1 and PA6/PP mass ratio = 1 : 4). [Color figure can be viewed in the online issue, which is available at wileyonlinelibrary.com.]

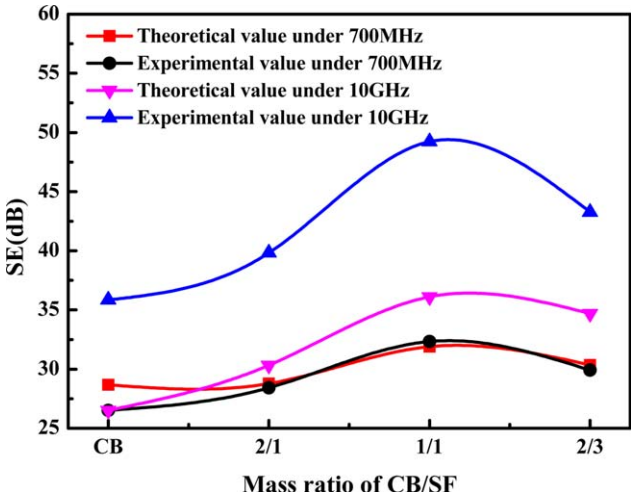

Figure 8. Comparison of the theoretical and experimental SEs of the CB/SF/PA6/PP composites with different CB/SF mass ratios (CB, 25 wt %; PA6/PP mass ratio = 1 : 4). [Color figure can be viewed in the online issue, which is available at wileyonlinelibrary.com.]

$$SE_A = 131.43T\sqrt{f\mu_r\sigma_r} \quad (2)$$

$$SE_R = 168.2 + 10\ \lg\left(\frac{\sigma_r}{f\mu_r}\right) \quad (3)$$

$$SE_{MR} = 10\lg\left[1 - 2\times10^{-0.1SE_A}\cos(0.23SE_A) + 10^{-0.2SE_A}\right] \quad (4)$$

where f, σ_r, d, μ_r, and T refer to the frequency of the electromagnetic wave (Hz), the electrical conductivity in relation to copper, the distance between interference source and material, the magnetic permeability in relation to the vacuum, and the relative thickness of material, respectively.

Figures 8 and 9 indicate the variations of the theoretical and experimental SEs of the CB/SF/PA6/PP composites under different CB/SF mass ratios and CBMSF content at fixed frequencies of 700 MHz and 10 GHz. When we made a comparison

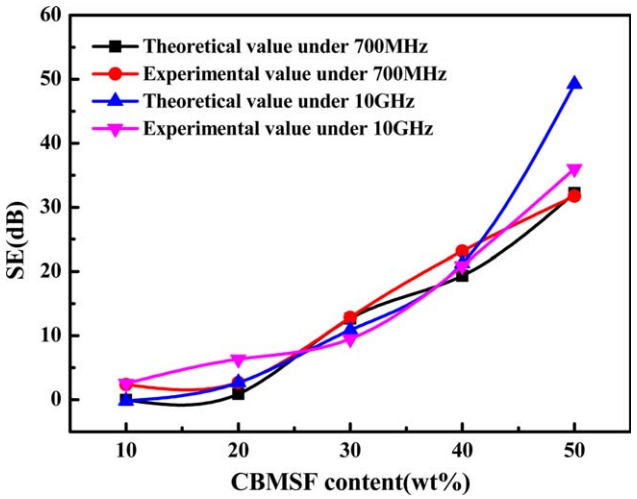

Figure 9. Comparison of the theoretical and experimental SEs of the CB/SF/PA6/PP composites with different CBMSF contents (CB/SF mass ratio = 1 : 1 and PA6/PP mass ratio = 1 : 4). [Color figure can be viewed in the online issue, which is available at wileyonlinelibrary.com.]

between the theoretical and experimental results in these two figures, we found that the difference was within 3 dB at 700 MHz. However, the difference was large when the frequency was 10 GHz. These differences were attributed to the simplification of the theoretical calculation equations.

CONCLUSIONS

Electrically conductive PA6/PP composites filled with the distributed CBMSF were successfully fabricated. We found that the addition of SF effectively decreased the percolation threshold of CB and increased the volume concentration of CB in the PA6/PP matrix. The EMI SE analysis showed that the addition of SF improved the SE of the composites. On the other hand, when the SF/CB mass ratio was 1 : 1, the best SE reached 38 dB (900 MHz) in the low-frequency range and 40.7 dB (16 GHz) in the high-frequency range.

Furthermore, the morphological observation also proved that CBMSF formed abundant conductive networks, and a conductive SF was achieved. The electrical conductivity and SE of the composites were significantly enhanced. Finally, Schelkunoff theory was used to predict the SE of the CB/SF/PA6/PP composites in the low-frequency range (from 400 MHz to 1 GHz). These results imply that filling PA6/PP with CBMSF is a simple and lower cost method for fabricating EMI shielding materials, and the CB/SF/PA6/PP composites exhibited potential as an EMI shielding material for civil SE demands.

ACKNOWLEDGMENTS

Financial support from the National Nature Science Foundation of China (contract grant number 51273068) is gratefully acknowledged.

REFERENCES

1. Geetha, S.; Satheesh Kumar, K. K.; Rao, C. R. K.; Vijayan, M.; Trivedi, D. C. J. *Appl. Polym. Sci.* **2009**, *112*, 2073.
2. Reena, V. L.; Sudha, J. D.; Ramakrishnan, R. *J. Appl. Polym. Sci.* **2013**, *128*, 1756.
3. Al-Saleh, M. H.; Sundararaj, U. *Macromol. Mater. Eng.* **2008**, *293*, 621.
4. Chung, D. D. L. *Carbon* **2001**, *39*, 279.
5. Ramoa, S. D.; Barra, G. M.; Oliveira, R. V.; Oliveira, M. G.; Cossa, M.; Soares, B. G. *Polym. Int.* **2013**, *62*, 1477.
6. Oh, J. H.; Oh, K. S.; Kim, C. G.; Hong, C. S. *Compos. B* **2004**, *35*, 49.
7. Madani, M. *J. Polym. Res.* **2010**, *17*, 53.
8. Im, J. S.; Kim, J. G.; Lee, Y. S. *Carbon* **2009**, *47*, 2640.
9. Tchoudakov, R.; Breuer, O.; Narkis, M. *Polym. Eng. Sci.* **1996**, *36*, 1336.
10. Chen, Z.; Brokken-Zijp, J. C. M.; Michels, M. A. J. *J. Polym. Sci. Part B: Polym. Phys.* **2006**, *44*, 33.
11. Dai, K.; Xu, X. B.; Li, Z. M. *Polymer* **2007**, *48*, 849.
12. Sina, N.; Hamid, G. *Compos. Sci. Technol.* **2007**, *67*, 3233.
13. Cui, L. M.; Zhang, Y.; Zhang, Y. X.; Zhang, X. F.; Zhou, W. *Eur. Polym. J.* **2007**, *43*, 5097.
14. Yang, Q. Q.; Liang, J. Z. *J. Appl. Polym. Sci.* **2010**, *117*, 1998.
15. Breuer, O.; Tchoudakov, R.; Narkis, M. *J. Appl. Polym. Sci.* **1997**, *64*, 1097.
16. Liu, Q. L.; Zhang, D.; Fan, T. X. *Carbon* **2008**, *46*, 461.
17. Bledzki, A. K.; Gassan, J. *Prog. Polym. Sci.* **1999**, *24*, 221.
18. Idicula, M.; Neelakantan, N. R.; Oommen, Z.; Joseph, K.; Thomas, S. J. *Appl. Polym. Sci.* **2005**, *96*, 1699.
19. Ahmed, K. S.; Vijayarangan, S. J. *Mater. Process. Technol.* **2008**, *207*, 330.
20. Towo, A. N.; Ansell, M. P. *Compos. Sci. Technol.* **2008**, *68*, 925.
21. Srekumar, P. A.; Saiter, J. M.; Joseph, K.; Unnikrishnan, G.; Thomas, S. *Compos. A* **2012**, *43*, 507.
22. Li, Y.; Mai, Y. W.; Ye, L. *Compos. Sci. Technol.* **2000**, *60*, 2037.
23. Feng, Y. H.; Shen, H. Z.; Qu, J. P.; Liu, B.; He, H. Z.; Han, L. Y. *Polym. Eng. Sci.* **2011**, *51*, 474.
24. Río, C. D.; Ojeda, M. C.; Acosta, J. L. *Eur. Polym. J.* **2000**, *36*, 1687.
25. Zhang, M. Q.; Yu, G.; Zeng, H. M.; Zhang, H. B.; Hou, Y. H. *Macromolecules* **1998**, *31*, 6724.
26. Dai, K.; Xu, X. B.; Li, Z. M. *Polymer* **2007**, *48*, 849.
27. He, H. Z.; Zhao, Y.; Wang, K. X.; He, X.; Zhou, H. Q.; Yao, Y. D.; Feng, Y. F. *Polym. Compos.* **2014**, *35*, 1038.
28. Li, Y.; Chen, C. X.; Zhang, S.; Ni, Y. W.; Huang, J. *Appl. Surf. Sci.* **2008**, *254*, 5766.
29. Li, Y.; Chen, C. X.; Li, J. T.; Zhang, S.; Ni, Y. W.; Cai, S.; Huang, J. *Nanoscale Res. Lett.* **2010**, *5*, 1170.
30. Lundgren, U.; Ekman, J.; Delsing, J. *IEEE Trans. Electromagn. C* **2006**, *48*, 766.
31. Feng, Y. H.; Li, Y. J.; Xu, B. P.; Zhang, D. W.; Qu, J. P.; He, H. Z. *Compos. B* **2013**, *44*, 193.
32. He, L. X.; Tjong, S. C. *Synth. Met.* **2012**, *161*, 2647.
33. Gupta, A.; Choudhary, V. *J. Mater. Sci.* **2011**, *46*, 6416.
34. Joo, J.; Lee, C. Y. *J. Appl. Phys.* **2000**, *88*, 513.
35. Paul, C. R. In Introuducion to Electromagnetic Compatibility; Chang, K., Ed.; Wiley: Hoboken, NJ, **2005**; Vol. *1*, Chapter 10, p 742.